



Hepatotoxicity Screening Taking a Mode-Of-Action Approach Using HepaRG Cells and HCA

Milena Mennecozzi, Brigitte Landesmann, Georgina Alexandra Harris, Roman Liska, and Maurice Whelan

European Commission, Joint Research Centre, Institute for Health and Consumer Protection, Ispra, Italy

Summary

The liver is central to the metabolism of xenobiotics. Evaluating the risk of liver toxicity is a major issue, and there is still no established in vitro screening strategy to reliably identify potentially hepatotoxic chemicals. In the approach described here, a mode-of-action targeted analysis of the literature has been used to identify toxicity pathways and the key biological events associated with them. This knowledge has then been used to design a multi-parametric high-throughput screening assay based on the quantification of fluorescently stained biomarkers expressed by treated HepaRG cells. Quantitative high-throughput screening was employed using a 96-well plate format, which facilitated the testing of a set of 92 reference chemicals with known hepatotoxic activity. We exposed HepaRG cells to 16-point serial concentrations to generate dose-response profiles. By determining the POD (point of departure), the test chemicals were then associated with different mode-of-action based categories.

Keywords: mode-of-action (MoA), HepaRG cells, high-content analysis (HCA), high-throughput screening (HTS), in vitro hepatotoxicity

1 Introduction

Liver toxicity is still a major problem for clinicians, pharmaceutical companies, and regulators (Andrade et al., 2005; Larrey, 2002; Lasser et al., 2002; Lee, 2003; Reuben et al., 2010). Intensive research is done worldwide to develop predictive *in vitro* screening systems with sufficient sensitivity and specificity. Reliable predictive *in vitro* tools would not only improve human public health by reducing exposure to unsafe drugs but also enhance animal welfare by replacing, refining, and reducing animal tests, thus providing an alternative to *in vivo* animal testing in human health risk assessment. Mode-of-action (MoA) is defined as “a description of key events or processes by which an agent causes a disease state or other adverse effect” (NRC, 2007, p. 38). Key events are measurable events that are critical to the induction of the toxicological response as hypothesized in the postulated MoA (Boobis et al., 2008; Sonich-Mullin et al., 2001; WHO Harmonization Project Document, 2007). Key events along this toxicological pathway also could be used to characterize the toxic potential of a chemical instead of using patho-physiologic categories such as apoptosis or necrosis, as well as to facilitate the assessment of other chemicals that share the same MoA.

At this point, the MoA for hepatotoxicity is not yet really defined. Some events, such as mitochondrial damage (Xu et al., 2008; Kaplowitz, 2002) and oxidative stress, seem to play a key role in various mechanisms of chemical-induced liver toxicity (Jaeschke et al., 2002). In this work, we focus our attention particularly on oxidative stress that is reported to be involved in toxic cell injury (Edwards and Preston, 2008; Guengerich and MacDonald, 2007; Kaplowitz, 2004; Liebler and Guengerich,

2005; Russmann et al., 2009; Simmons et al., 2009). We tested the crucial role of oxidative stress in hepatotoxicity, exposing HepaRG cells to 92 chemicals with known hepatotoxic effects. HepaRG is a metabolically competent hepatic cell model (Anthérieu et al., 2010), derived from a liver tumor of a female suffering from hepatocellular carcinoma (Gripon et al., 2002). These cells, seeded at high confluence in the presence of 2% DMSO, insulin, and hydrocortisone differentiate into hepatocyte-like cells resembling primary hepatocytes and biliary epithelial cells (Cerec et al., 2007). Differentiated HepaRG cells express phase II enzymes, nuclear receptors, transporters (Le Vee et al., 2006), liver-specific protein (Guillouzo et al., 2007) and various CYPs (Aninat et al., 2006; Turpeinen et al., 2009; Anthérieu et al., 2010). Oxidative stress was tested in these cells by measuring the formation of reactive oxygen species (ROS). In the same cell, a multiparametric analysis allowed the collection of information on cell loss, nuclear area, and nuclear intensity. The test chemicals were grouped consecutively according to their effect on ROS formation, viability, and DNA condensation. The results from this cell-based assay could ultimately be used to prioritize chemicals according to their potential liver toxicity.

2 Materials and methods

Chemicals and supplies

HepaRG cells were obtained from Biopredic International (Rennes, France) and stored in liquid nitrogen. William's E medium, L-glutamine, penicillin/streptomycin, and trypsin-EDTA were acquired from Invitrogen. Insulin and hydrocortisone



were purchased from Sigma-Aldrich. HyClone Fetalclone III serum, Hoechst and DHE dyes were from Thermo Scientific. The 96-well clear bottom black polystyrene microplates were from Corning. Test drugs and chemicals were purchased from Sigma-Aldrich. Stock solutions were prepared in DMSO for all test compounds.

Cell culture and differentiation

Human hepatocellular carcinoma cells HepaRG were cultured in William's E medium supplemented with 10% serum, 1% L-glutamine, 1% penicillin/streptomycin, 5 µg/ml bovine insulin and 50 µM hydrocortisone hemisuccinate. The cells were seeded at a density of 4×10^6 cells in 150 cm² flasks and the medium was refreshed every two days. After two weeks, 2% DMSO was added to the culture medium to stimulate differentiation. Differentiation medium was changed every 2 days for two weeks. Finally, the differentiated cells were gently harvested with trypsin-EDTA and seeded into 96-well clear bottom black plates at a density of 50,000 cells/well using the STARlet Hamilton platform.

Treatment with test compounds

All chemicals were initially solubilized in 100% DMSO. They were then diluted in culture medium (described above) but with 5% serum. Quantitative high-throughput screening (qHTS) (Inglese et al., 2006) format was used. To assess hepatotoxicity, the HepaRG cells were exposed to 92 chemicals at 16 concentrations (see Tab. 1) and incubated at 37°C, 5% CO₂, 100% humidity for 72 h. In each plate, 4 negative control wells (cells treated with only DMSO) were included. The experiment consists of three independent biological repeats in which different cell batches were used on different days. All the treatment procedures were completely automated and the entire process was managed by Hamilton software.

Staining and endpoint measurements

Chemically treated HepaRG cells were stained for 30 min using an oxidative stress staining kit (Thermo Scientific) containing dihydroethidium (DHE) and Hoechst 33342 dye. After 30 min in the incubator at 37°C, 5% CO₂, 100% humidity, the cells were fixed with 4% formaldehyde (Sigma) for 20 min at room temperature. Finally cells were washed twice with PBS (Invitrogen) and imaged via a high-content analysis approach (HCA) using Cellomics ArrayScan vTi. A 10x objective was used to collect 10 image fields per well for two fluorescence channels with the XF93 filter set. Cell count, nuclear area, nuclear intensity, and ROS formation (DHE intensity) parameters were collected using the Target Activation Bioapplication v.4 from Cellomics Scan Software.

Data analysis

Statistical analysis was performed using Matlab 7.5. software for Windows. The raw response data, obtained after cellular exposure to the different compound concentrations, were adjusted as follows. First, the mean and standard deviation (SD) were calculated for the negative control samples. The normalization

of the data was performed by subtracting the calculated mean from each data point and dividing by the SD. The adjusted results were plotted against concentration as an average over three biological replicates. Upper and lower boundaries (three times the SD) were set to define the point of departure (POD). The POD is identified as: A) the first concentration at which a permanent exit from the defined boundaries occurs or B) the lowest concentration for which temporary exit occurs. PODs were identified for each endpoint being analyzed (cell count, nuclear area, nuclear intensity, ROS formation) as displayed in Figures 4 and 5. A heat map was generated using MeV v4.7 (MultiExperiment Viewer), software available online.

3 Results

MoA-drug induced hepatotoxicity hypothesis

Looking at the various described pathways that lead to different features of toxic liver damage, three events are observed in all pathogenic processes, which therefore can be called key events: metabolic activation, oxidative stress, and mitochondrial damage (Xu et al., 2008; Jaeschke et al., 2002; Russmann et al., 2009; Kaplowitz, 2002; Malhi and Gores, 2008). Once a chemical arrives at the liver it is metabolized there. The metabolic alteration may inactivate the chemical or it may result in the production of an active metabolite. Subsequently, the toxic effects are caused, likewise, by either the parent drug or the reactive metabolite (Park et al., 2005). Using a mode-of-action targeted analysis of the existing literature, we made a hypothesis of MoA for hepatotoxicity (Fig. 1). A parent chemical/metabolite can cause:

- a) *Oxidative stress*. Chemical metabolism can produce reactive oxygen species, reactive lipid peroxidation, and GSH depletion. This chain reaction can trigger mitochondrial damage (Jaeschke and Ramachandran, 2011).
- b) *Mitochondrial dysfunction*. Metabolites can directly bind to mitochondrial proteins, causing direct toxicity via inhibition of the respiratory chain. Damaged mitochondria and β -oxidation increase ROS formation leading to oxidative stress (Russmann et al., 2009).
- c) *Protein adduct formation*. Protein covalent adducts formed after exposure to xenobiotic, activate T cells and induce the release of cytokines, causing immune responses (Yang et al., 2006; Zhang et al., 2011). Consecutive inflammatory processes then contribute to oxidative stress and mitochondrial damage (Adams et al., 2010).
- d) *Activation of non-parenchymal liver cells*. Non-parenchymal liver cells exposed to chemicals produce ROS, induce oxidative stress, and induce mitochondrial damage via inflammation, cytokine release, and fibrosis (pathway not shown in Fig. 1) (Poli, 2000).
- e) *Inhibition of bile transporter systems*. Either metabolites or parent chemicals can cause cholestasis through the inhibition of bile transport systems and, consequently, induce inflammation, oxidative stress, and mitochondrial damage (Copple et al., 2010; Pauli-Magnus and Meier, 2006).

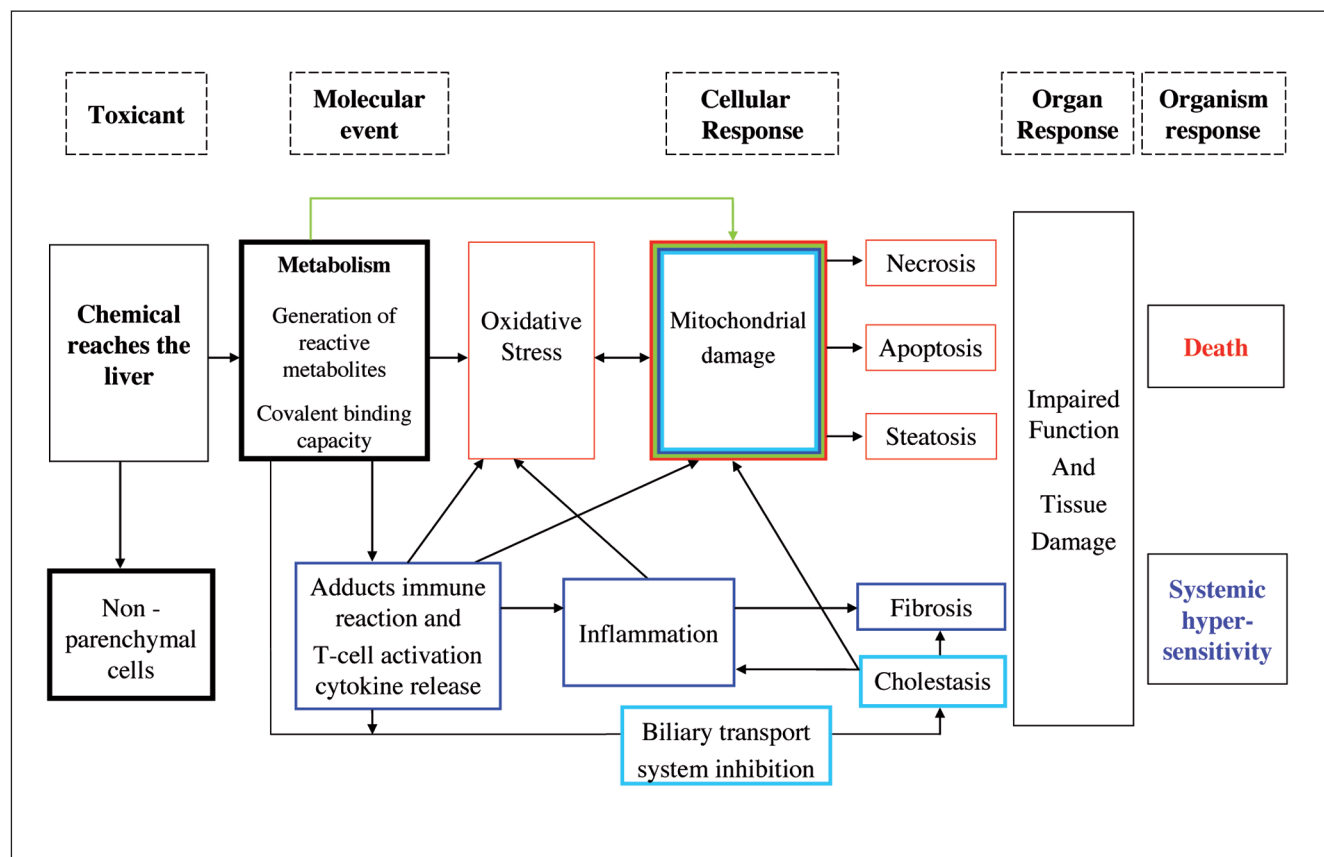


Fig. 1: Diagram representing the mode-of-action proposed in which oxidative stress and mitochondrial damage plays a key role in the different known mechanisms of hepatotoxicity

Extensive literature research has lead to the proposed hypothesis that oxidative stress plays a crucial role in various hepatotoxicity pathways. This key event can therefore be used as a marker for potential chemical induced hepatotoxicity.

These processes can cause various types of liver injury, namely hepatitis, necrosis, (Lemasters et al., 1999), steatosis, cholestasis (Pauli-Magnus and Meier, 2006), and fibrosis/cirrhosis.

Chemical selection

Taking into consideration several chemical libraries, including ToxCast 320, we decided to select some chemicals that are known or suspected to be hepatotoxic. In the chemical selection step we excluded all the volatile chemicals, and we prioritized the substances that were commercially available and soluble in DMSO. A total of 92 chemicals were selected, including drugs such as troglitazon, tamoxifen, and nilutamide, and pesticides (phenotrin, phrallertin, cyfluthrin, etc.) (Tab.1). The choice of these chemicals is envisioned to cover different toxicity pathways. Four non-hepatotoxic chemicals (propyl 4-hydroxybenzoate, DL-thyroxine, potassium chloride, and dibutyl phthalate) were included in the list. Rotenone was used as positive control for reactive oxygen species formation. As negative control, the HepaRG cells were treated with vehicle (DMSO). The cell treatment was performed using a concentration range of 1×10^{-4} M up to 1.5×10^{-9} M. If no effects were obtained at 1×10^{-4} M, the dose of many of these chemicals

was increased 5- to 10-fold. For a few chemicals, the dose was reduced 5- to 10-fold because precipitation was observed in the medium.

HepaRG high-content analysis

After treating two-week-old differentiated HepaRG and staining them with two fluorescent probes (Fig. 2), we were able to measure signals that are directly linked to the hypothetical key events of hepatotoxicity described in Figure 1. Hoechst and DHE fluorescence staining were quantified using high-content imaging. Automated imaging analysis performed with Cellomics ArrayScan vTi and Cellomics Scan software was used to measure cell viability, nuclear area and intensity, and ROS formation. Typical morphological and toxic changes are shown in Figure 3. Rotenone produced a marked reduction in cell number and nuclear area but an increase in ROS fluorescence signal and nuclear intensity (DNA condensation). This multiparametric analysis allowed the investigation of the possible mechanism by which a chemical exerts its hepatotoxicity and whether this is led by the production of ROS. In Figure 4, the dose response curves are reported for a representative set of six chemicals, i.e., amiodarone hydrochloride, troglitazone, ro-

**Tab. 1: Selected reference chemicals**

The selected chemicals with their corresponding CAS number and concentrations at which each were tested are reported in the following table.

Compound	CAS #	Tested <i>in vitro</i> concentration range (M)
Carbamazepine	298-46-4	1.5×10^{-9} - 1×10^{-4}
Kaempferol	520-18-3	1.5×10^{-9} - 1×10^{-4}
1,2-dichlorobenzene	95-50-1	1.5×10^{-8} - 1×10^{-3}
Phthalic anhydride	85-44-9	1.5×10^{-8} - 1×10^{-3}
Triticonazole	131983-72-7	7.6×10^{-10} - 5×10^{-5}
Thiabendazole	148-79-8	7.6×10^{-10} - 5×10^{-5}
Vinclozolin	50471-44-8	1.5×10^{-9} - 1×10^{-4}
Fluometuron	2164-17-2	1.5×10^{-9} - 1×10^{-4}
Phenothrin	26002-80-2	1.5×10^{-8} - 1×10^{-3}
Chloramphenicol	56-75-7	1.5×10^{-8} - 1×10^{-3}
Quizalofop-ethyl	76578-14-8	1.5×10^{-8} - 1×10^{-3}
Atropine sulfate salt monohydrate	5908-99-6	1.5×10^{-8} - 1×10^{-3}
Pentachlorobenzene	608-93-5	1.5×10^{-9} - 1×10^{-4}
Bisphenol A	80-05-7	1.5×10^{-9} - 1×10^{-4}
Acetaminophen	103-90-2	1.5×10^{-8} - 1×10^{-3}
Tralkoxydim	87820-88-0	1.5×10^{-8} - 1×10^{-3}
Perfluorooctanesulfonic acid	1763-23-1	1.5×10^{-8} - 1×10^{-3}
Trans-Nonachlor	39765-80-5	7.6×10^{-9} - 5×10^{-4}
Alachlor	15972-60-8	1.5×10^{-9} - 1×10^{-4}
Diquat dibromide monohydrate	6385-62-2	1.5×10^{-8} - 1×10^{-3}
Methyl viologen dichloride hydrate	1910-42-5	1.5×10^{-8} - 1×10^{-3}
Zoxamide	156052-68-5	7.6×10^{-9} - 5×10^{-4}
Etridiazole	2593-15-9	1.5×10^{-8} - 1×10^{-3}
Fluazinam	79622-59-6	1.5×10^{-9} - 1×10^{-4}
Copper sulphate	7758-98-7	1.5×10^{-8} - 1×10^{-3}
Terbutryn	886-50-0	7.6×10^{-9} - 5×10^{-4}
Ibuprofen	15687-27-1	1.5×10^{-8} - 1×10^{-3}
Phenytoin	57-41-0	7.6×10^{-9} - 5×10^{-4}
Chloridazon	1698-60-8	1.5×10^{-8} - 1×10^{-3}
Methidathion	950-37-8	1.5×10^{-8} - 1×10^{-3}
Fenarimol	60168-88-9	1.5×10^{-9} - 1×10^{-4}
Oxyfluorfen	42874-03-3	7.6×10^{-9} - 5×10^{-4}
Endosulfan (alpha)	959-98-8	1.5×10^{-8} - 1×10^{-3}
Cycloheximide	66-81-9	7.6×10^{-9} - 5×10^{-4}
Benzo[a]Pyrene	50-32-8	1.5×10^{-10} - 1×10^{-5}
Dazomet	533-74-4	1.5×10^{-8} - 1×10^{-3}
Triclosan	3380-34-5	7.6×10^{-9} - 5×10^{-4}
Nilutamide	63612-50-0	1.5×10^{-9} - 1×10^{-4}
Captafol	2425-06-1	7.6×10^{-9} - 5×10^{-4}
Acetochlor	34256-82-1	1.5×10^{-8} - 1×10^{-3}
Diethylstilbestrol	56-53-1	1.5×10^{-9} - 1×10^{-4}
Flutamide	13311-84-7	1.5×10^{-9} - 1×10^{-4}
Tamoxifen	10540-29-1	7.6×10^{-9} - 5×10^{-4}
Chlorpromazine hydrochloride	69-09-0	7.6×10^{-9} - 5×10^{-4}
Amiodarone hydrochloride	19774-82-4	1.5×10^{-9} - 1×10^{-4}
Cyhalothrin (@Karate)	91465-08-6	1.5×10^{-8} - 1×10^{-3}
METHYLMERCURY(II) CHLORIDE	115-09-3	7.6×10^{-9} - 5×10^{-4}
Permethrin	52645-53-1	1.5×10^{-8} - 1×10^{-3}
Strychnidin-10-one, 2,3-dimethoxy-aldrin	357-57-3	1.5×10^{-8} - 1×10^{-3}

Compound	CAS #	Tested <i>in vitro</i> concentration range (M)
Aldrin	309-00-2	7.6×10^{-9} - 5×10^{-4}
Acetylsalicylic acid	50-78-2	1.5×10^{-8} - 1×10^{-3}
Dinoseb	88-85-7	1.5×10^{-8} - 1×10^{-3}
Flusilazole	85509-19-9	7.6×10^{-9} - 5×10^{-4}
Cyproconazol	94361-06-5	7.6×10^{-9} - 5×10^{-4}
Cypermethrin	52315-07-8	1.5×10^{-8} - 1×10^{-3}
Cyfluthrin	68359-37-5	1.5×10^{-8} - 1×10^{-3}
Bisphenol A diglycidyl ether	1675-54-3	1.5×10^{-8} - 1×10^{-3}
Pendimethalin	40487-42-1	1.5×10^{-8} - 1×10^{-3}
Pyriproxyfen	95737-68-1	1.5×10^{-8} - 1×10^{-3}
Lactofen	77501-63-4	1.5×10^{-8} - 1×10^{-3}
Sodium dodecyl sulfate	151-21-3	1.5×10^{-8} - 1×10^{-3}
Warfarin	81-81-2	1.5×10^{-9} - 1×10^{-4}
Verapamil hydrochloride	152-11-4	1.5×10^{-8} - 1×10^{-3}
Propiconazole	60207-90-1	7.6×10^{-9} - 5×10^{-4}
2-Acetamidofluorene	53-96-3	7.6×10^{-9} - 5×10^{-4}
Myclobutanil	88671-89-0	7.6×10^{-9} - 5×10^{-4}
Fludioxonil	131341-86-1	7.6×10^{-9} - 5×10^{-4}
Hexaconazol	79983-71-4	7.6×10^{-9} - 5×10^{-4}
Perfluorooctanoic acid	335-67-1	1.5×10^{-8} - 1×10^{-3}
Omeprazole	73590-58-6	1.5×10^{-8} - 1×10^{-3}
Nitrofen	1836-75-5	1.5×10^{-8} - 1×10^{-3}
Troglitazone	97322-87-7	1.5×10^{-9} - 1×10^{-4}
Haloperidol	52-86-8	1.5×10^{-9} - 1×10^{-4}
S-Bioallethrin	28434-00-6	1.5×10^{-8} - 1×10^{-3}
Prallethrin	23031-36-9	1.5×10^{-8} - 1×10^{-3}
Imazalil	35554-44-0	7.6×10^{-9} - 5×10^{-4}
Thiophanate-methyl	23564-05-8	1.5×10^{-8} - 1×10^{-3}
Pentachlorophenol	87-86-5	1.5×10^{-9} - 1×10^{-4}
Cadmium chloride	10108-64-2	1.5×10^{-9} - 1×10^{-4}
Rotenone	83-79-4	1.5×10^{-9} - 1×10^{-4}
Strychnine	57-24-9	1.5×10^{-9} - 1×10^{-4}
Bis(2-ethylhexyl) phthalate	117-81-7	1.5×10^{-8} - 1×10^{-3}
dimethylcarbamoyl chloride	79-44-7	1.5×10^{-8} - 1×10^{-3}
Norflurazon	27314-13-2	1.5×10^{-9} - 1×10^{-4}
4-Nitrotoluene	99-99-0	1.5×10^{-8} - 1×10^{-3}
Simazine	122-34-9	1.5×10^{-9} - 1×10^{-4}
2-Propylpentanoic acid	99-66-1	1.5×10^{-9} - 1×10^{-4}
Dibutyl phthalate	84-74-2	1.5×10^{-9} - 1×10^{-4}
Propyl 4-hydroxybenzoate	94-13-3	1.5×10^{-9} - 1×10^{-4}
Genistein	446-72-0	1.5×10^{-9} - 1×10^{-4}
DL-thyroxin	51-48-9	1.5×10^{-9} - 1×10^{-4}
Potassium Chloride	7447-40-7	1.5×10^{-9} - 1×10^{-4}

tenone, cycloheximide, acetaminophen, and dibutyl-phthalate. In accordance with what is known about the mechanisms of liver toxicity, amiodarone hydrochloride (Spaniol et al., 2001; Waldhauser et al., 2006) (Fig. 4A), troglitazone (Narayanan et al., 2003; Uetrecht, 2010) (Fig. 4B), and rotenone (Terzi et al., 2004) (Fig. 4C) caused oxidative stress at low concentration. Chemicals such as cycloheximide (Fig. 4D) induced cell death, as previously reported, but no ROS formation was ob-

served (Alessenko et al., 1997; Sánchez et al., 1997). Other chemicals, such as acetaminophen, a well-known oxidative stress inducer compound, showed an increase of ROS formation at a lower dose than the concentration at which an effect on cell viability is observed (Fig. 4E) (McGill et al., 2011). Dibutyl-phthalate was non-toxic at the tested concentration in HepaRG cells (Fig. 4F). Figure 5 shows a summary of our multiparametric analysis results. The lowest concentration at

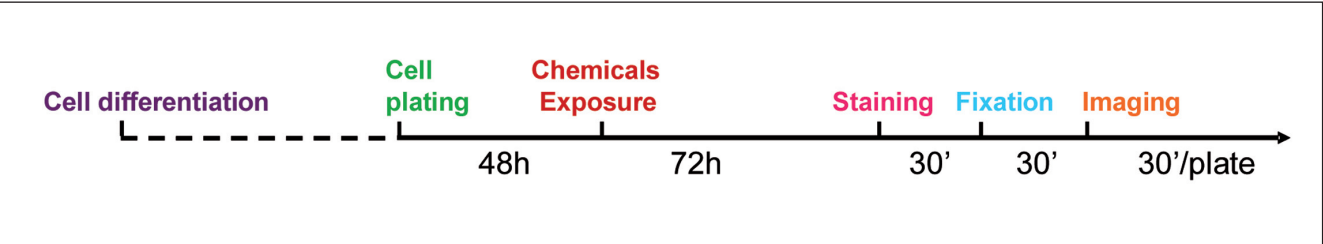


Fig. 2: Steps involved in the 92 selected chemicals screening
Two week-old confluent differentiated HepaRG cells were seeded in 96 well plates and then treated for 72 h with serial dilutions of 92 chemicals. Treated cells were stained with two fluorescent dyes: Hoechst and DHE fixed with 4% formaldehyde and imaged using Cellomics Arrayscan vTi.

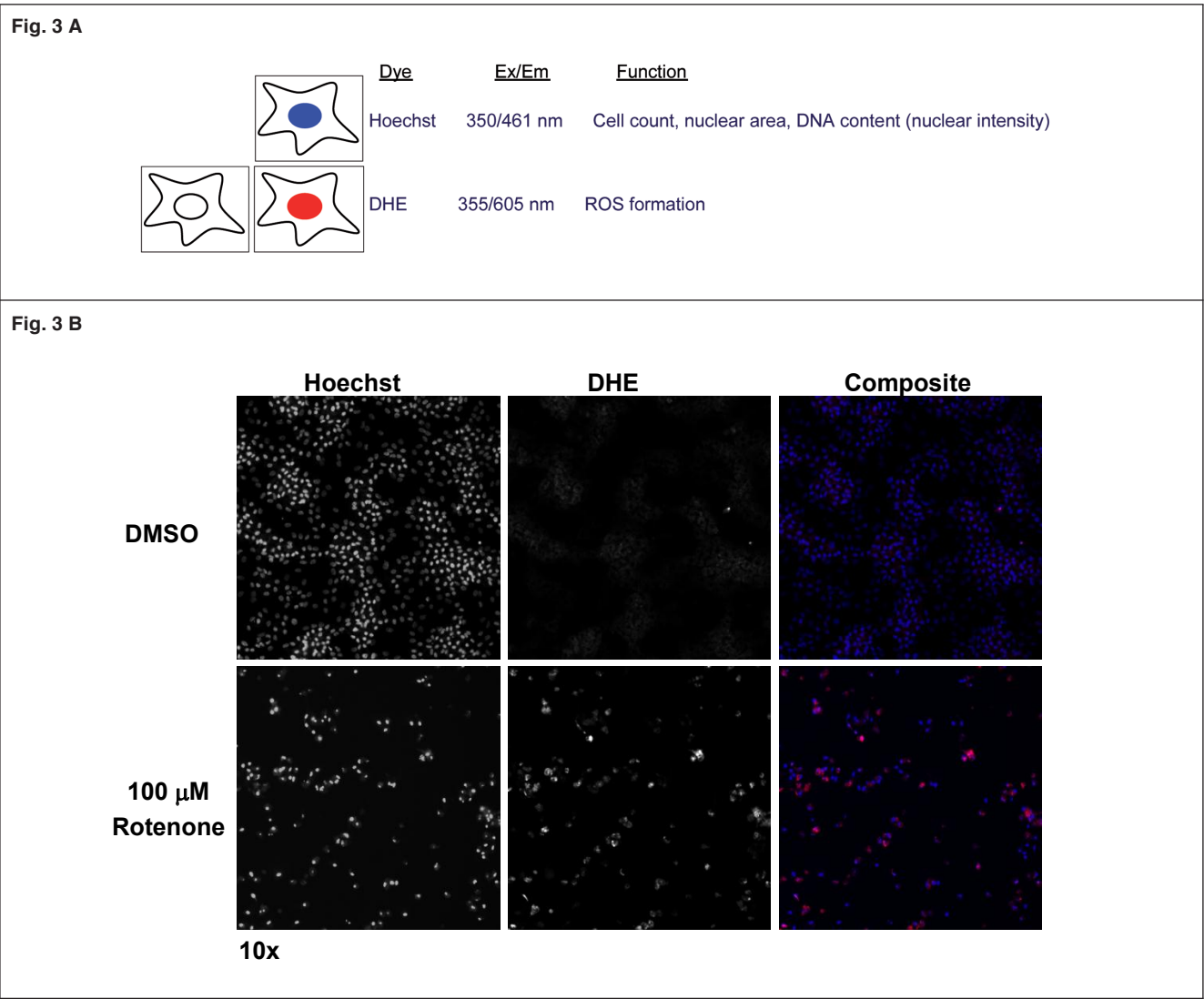


Fig. 3: High-content analysis on HepaRG cells
A) Hoechst dye was used to stain the cell nuclei and dihydroethidium (DHE) oxidation was employed to measure production of ROS. In the presence of reactive oxygen species, DHE is oxidised to give a fluorescent ethidium product able to intercalate with DNA.
B) Comparative DHE signal observed using fluorescent imaging after cells are exposed to vehicle control (DMSO) and 100 μM Rotenone (positive control for oxidative stress) for 72 h. The control well shows densely populated hepatocyte colonies with low DHE signal while rotenone-treated cells are reduced in number and size, and show increased nuclear and red DHE signal (in the composite) intensity.

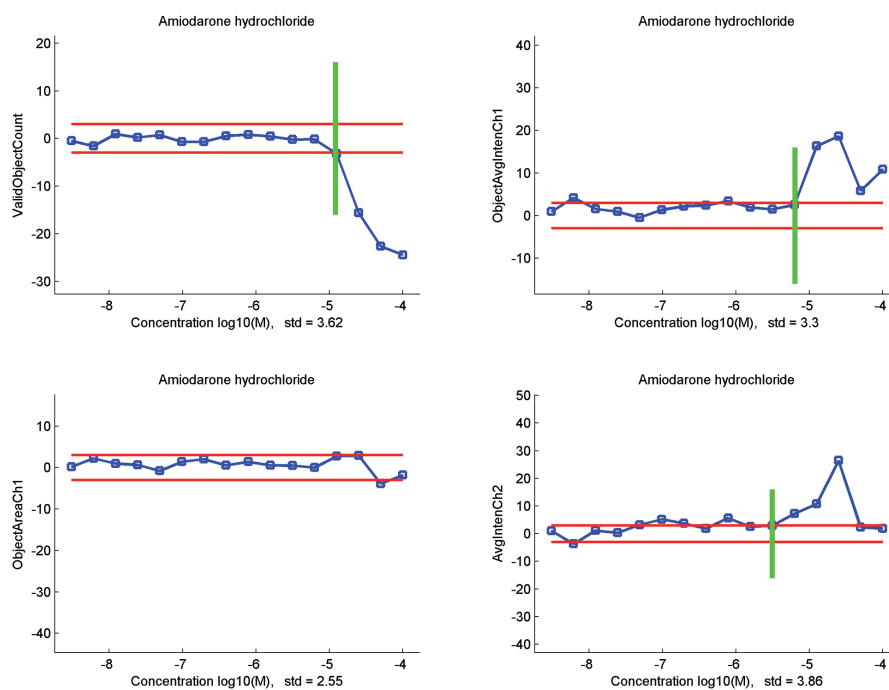
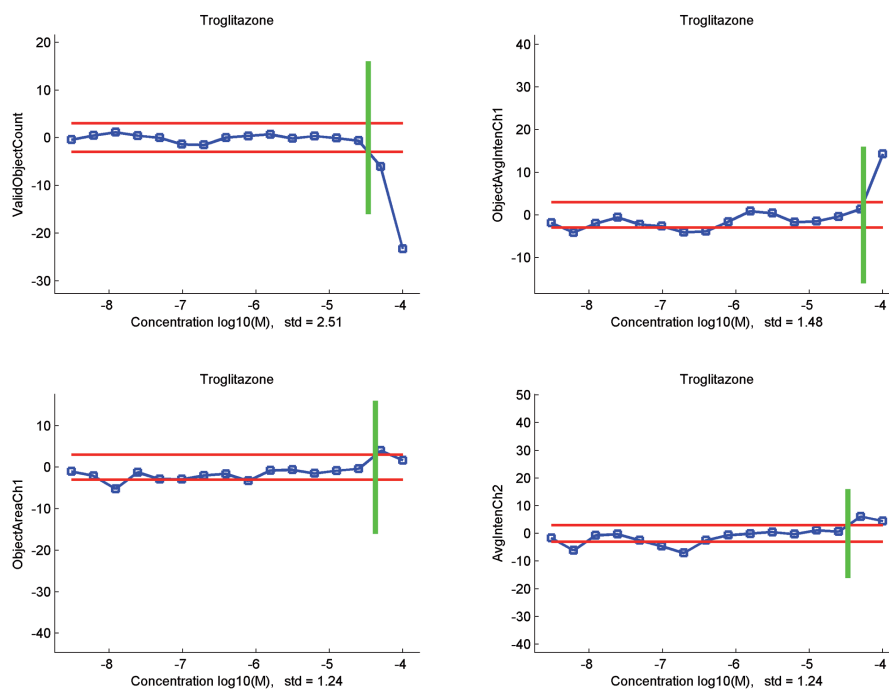
Fig. 4 A

Fig. 4 B




Fig. 4 C

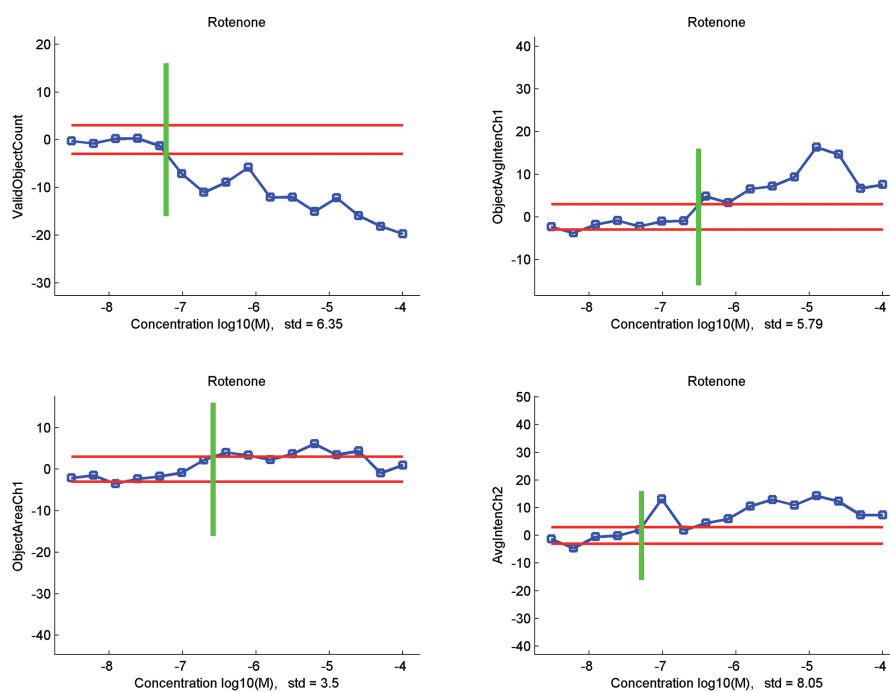


Fig. 4 D

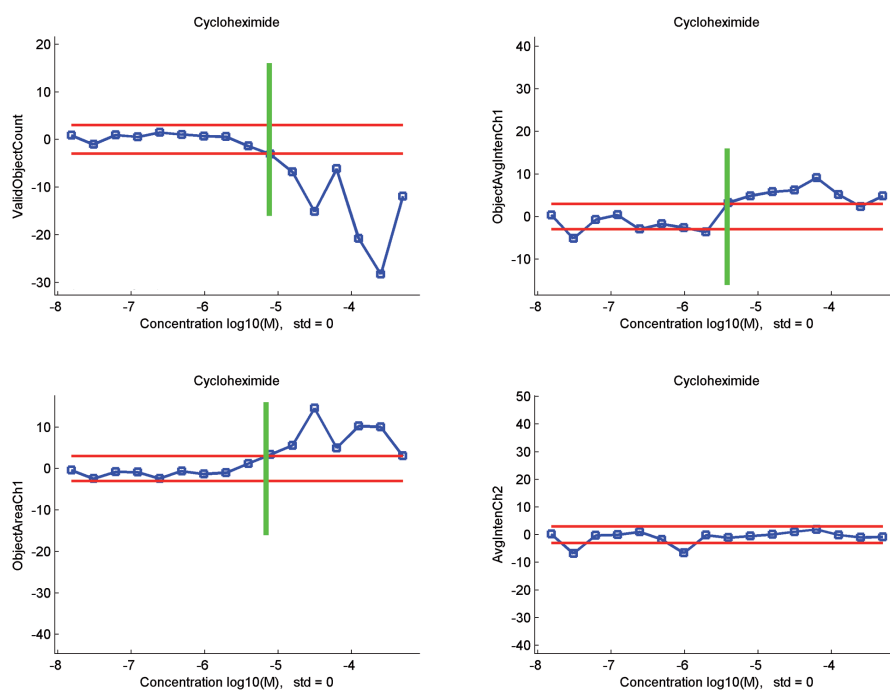


Fig. 4 E

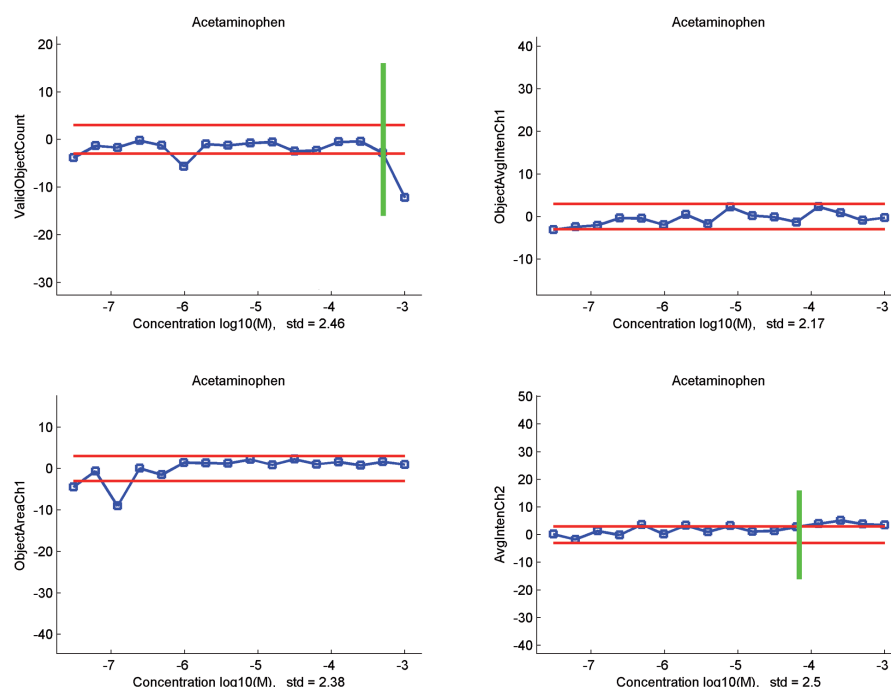
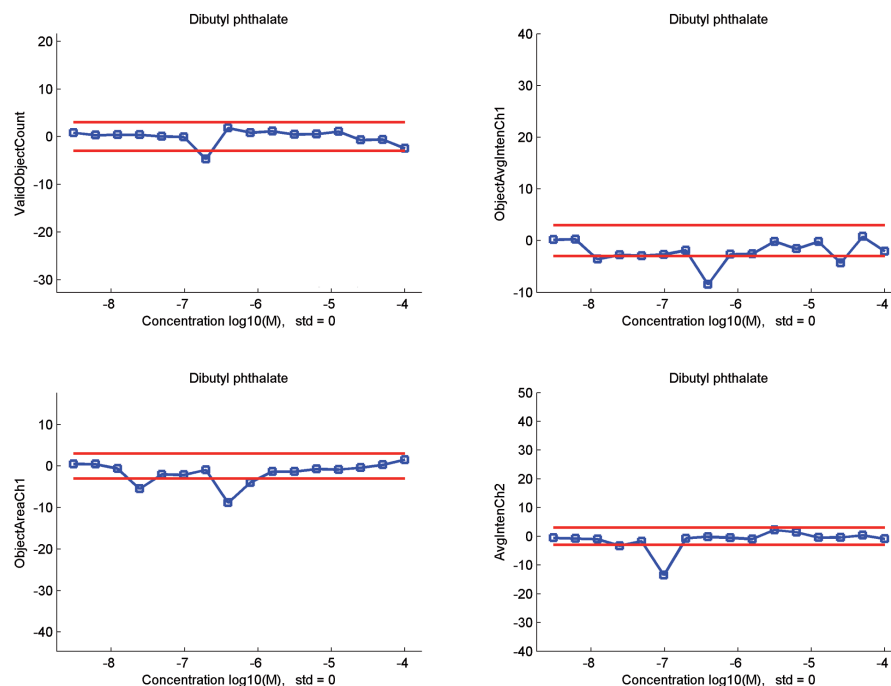
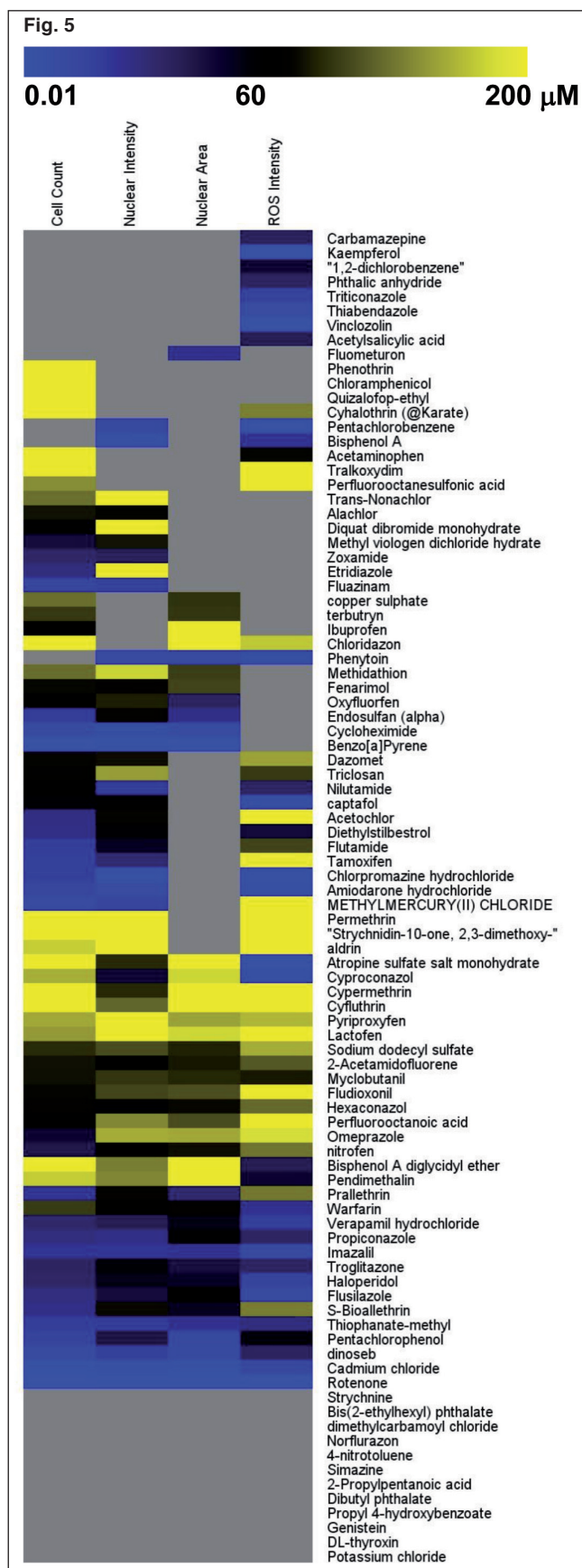


Fig. 4 F


Fig. 4: Effects of HepaRG exposure to chemicals

48 h after seeding, cells were treated with chemicals for 72 h. Results are means of three biological repeats. Intensity of nuclear and ROS markers was measured as an average of the overall cell population and PODs were determined (see data analysis methods section). Quantification by imaging analysis indicates that at higher concentrations amidarone hydrochloride (A) and troglitazone (B) induce ROS but have no effect on cell viability. (C) As expected, rotenone, used as a positive control, has a clear positive result for all four tested endpoints. (D) Cycloheximide is an example where toxicity, observed as a decrease in cell count and changes in nuclear morphology, does not show a relationship with an increase in ROS. (E) Lower concentrations of acetaminophen increase ROS signal and have an effect on cell viability only at higher concentrations. (F) No response was obtained treating HepaRG cells for 72 h with dibutyl phthalate.



which a POD was calculated for any of the parameters measured was used to profile the test chemicals. We used a scale of colors from yellow to light blue to specify the concentration at which there is a response compared to control. This allowed us to identify and group together those chemicals with a similar response. Chemicals with similar profiles may likely have a common hepatotoxicity MoA. We observed that rotenone, cadmium chloride, and imazalil affected all 4 tested parameters at a dose lower than 20 μM . Also, omeprazole, perfluorooctanoic acid, fludioxonil, lactofen, pyriproxyfen, cypermethrin, and cyfluthrin induced generation of ROS, DNA condensation, and cell loss, but only at higher doses. Some chemicals, such as carbamazepine, kaempferol, 1,2-dichlorobenzene, phthalic anhydride, triticonazole, thiabendazole, vinclozolin, acetylsalicylic acid, pentachlorobenzene, and bisphenol A formed ROS but no cell loss was observed. At 72 h exposure, phenothrin, chloramphenicol, quizalofop-ethyl, trans-nonachlor, alachlor, diquat dibromide monohydrate, methyl viologen dichloride hydrate, zoxamide, etridiazole, fluazinam, copper sulphate, terbutryn, ibuprofen, methidathion, fenarimol, oxyfluorfen, endosulfan, cycloheximide and benzo-a-pyrene demonstrated toxicity not associated with ROS formation. For these chemicals earlier time points need to be analyzed. On the other hand, 12 chemicals (see gray cells in Fig. 5) were not toxic at the tested concentrations.

4 Discussion

The goal of this work is to design an *in vitro* testing strategy to identify chemicals that are potentially hepatotoxic in humans, to associate them with specific MoA categories, and to group them accordingly. To begin with, we tested oxidative stress in HepaRG treated with various hepatotoxic chemicals which provided us with insights towards ROS-mediated toxicity and MoA-driven chemical testing.

The metabolically competent HepaRG cell line is a very attractive alternative model for *in vitro* hepatotoxicity testing. Our cell-based screening of 92 chemicals showed that this cell model is a promising alternative to either primary hepatocytes or other human tumor hepatic cell lines. Moreover, the HepaRG are easy to grow and to cryo-preserve.

In this work we have proven that automated cell imaging and HCA are feasible using the human hepatoma cell line HepaRG. Furthermore, the HCA offers significant advantages over traditional HTS assays without compromising throughput. As already

Fig. 5: Clustering of *in vitro* multiparametric analysis results for 92 test chemicals

Target Activation Bioapplication v.4 from Cellomics Scan software was used to obtain data on four parameters: cell count, nuclear intensity, nuclear area and ROS intensity. Following analysis, the chemicals were characterized to determine the concentration at which a positive result is observed for each endpoint. The different colours specify the concentration at which there is a response compared to control.

reported, using image analysis algorithms many more parameters can be tested in the same hepatic cells (O'Brien et al., 2006), thus increasing the information content obtained from a single assay.

Our hypothesis-driven MoA-based approach to design a testing strategy for *in vitro* hepatotoxicity is feasible and efficient but remains challenging. The identification and measurement of additional relevant MoA associated biomarkers for studying hepatotoxicity is needed. Bile salt transport (BSEP) inhibition, mitochondrial damage, and glutathione depletion are some of the key biological events that should be incorporated into our battery of screening tests. In this preliminary study, only 72 h responses have been measured. Future time course experiments will further elucidate the role of ROS in MoA associated with liver toxicity. Importantly, the concentrations applied in cell culture should be put into context with human exposure to determine the relevance of the toxicity observed with some chemicals. Moreover, metabonomics and transcriptomics studies, anchored with HCA, will help to refine and reinforce a MoA description of hepatotoxicity.

References

- Adams, D. H., Ju, C., Ramaiah, S. K., et al. (2010). Mechanisms of immune-mediated liver injury. *Toxicol. Sci.* 115, 307-321.
- Alessenko, A. V., Boikov, P. Y., Filippova, G. N., et al. (1997). Mechanisms of cycloheximide-induced apoptosis in liver cells. *FEBS Lett.* 416, 113-116.
- Andrade, R. J., Lucena, M. I., Fernández, M. C., et al. (2005). Drug-induced liver injury: an analysis of 461 incidences submitted to the Spanish registry over a 10-year period. *Gastroenterology* 129, 512-521.
- Aninat, C., Piton, A., Glaize, D., et al. (2006). Expression of cytochromes P450, conjugating enzymes and nuclear receptors in human hepatoma HepaRG cells. *Drug Metab. Dispos.* 34, 75-83.
- Anthérieu, S., Chesné, C., Li, R., et al. (2010). Stable expression, activity, and inducibility of cytochromes P450 in differentiated HepaRG cells. *Drug Metab. Dispos.* 38, 516-525.
- Boobis, A. R., Doe, J. E., Heinrich-Hirsch, B., et al. (2008). IPCS framework for analyzing the relevance of a noncancer mode of action for humans. *Crit. Rev. Toxicol.* 38, 87-96.
- Cerec, V., Glaize, D., Garnier, D., et al. (2007). Transdifferentiation of hepatocyte-like cells from the human hepatoma HepaRG cell line through bipotent progenitor. *Hepatology* 45, 957-967.
- Copple, B. L., Jaeschke, H., and Klaassen, C. D. (2010). Oxidative stress and the pathogenesis of cholestasis. *Semin. Liver Dis.* 30, 195-204.
- Edwards, S. W. and Preston, R. J. (2008). Systems biology and mode of action based risk assessment. *Toxicol. Sci.* 106, 312-318.
- Gripon, P., Rumin, S., and Urban, S. (2002). Infection of a human hepatoma cell line by hepatitis B virus. *Proc. Natl. Acad. Sci. USA* 99, 15655-15660.
- Guengerich, F. P. and MacDonald, J. S. (2007). Applying mechanisms of chemical toxicity to predict drug safety. *Chem. Res. Toxicol.* 20, 344-369.
- Guillouzo, A., Corlu, A., Aninat, C., et al. (2007). The human hepatoma HepaRG cells: a highly differentiated model for studies of liver metabolism and toxicity of xenobiotics. *Chem. Biol. Interact.* 168, 66-73.
- Inglese, J., Auld, D. S., Jadhav, A., et al. (2006). Quantitative high-throughput screening: a titration-based approach that efficiently identifies biological activities in large chemical libraries. *Proc. Natl. Acad. Sci. USA* 103, 11473-11478.
- Jaeschke, H., Gores, G. J., Cederbaum, A. I., et al. (2002). Mechanisms of hepatotoxicity. *Toxicol. Sci.* 65, 166-176.
- Jaeschke, H. and Ramachandran, A. (2011). Reactive oxygen species in the normal and acutely injured liver. *J. Hepatol.* 55, 227-228.
- Kaplowitz, N. (2002). Biochemical and cellular mechanisms of toxic liver injury. *Semin. Liver Dis.* 22, 137-144.
- Kaplowitz, N. (2004). Drug-induced liver injury. *Clin. Infect. Dis.* 1, 38.
- Larrey, D. (2002). Epidemiology and individual susceptibility to adverse drug reactions affecting the liver. *Semin. Liver Dis.* 22, 145-155.
- Lasser, K. E., Allen, P. D., Woolhandler, S. J., et al. (2002). Timing of new black box warnings and withdrawals for prescription medications. *JAMA* 287, 2215-2220.
- Le Vee, M., Jigorel, E., Glaize, D., et al. (2006). Functional expression of sinusoidal and canalicular hepatic drug transporters in the differentiated human hepatoma HepaRG cell line. *Eur. J. Pharm. Sci.* 28, 109-117.
- Lee, W. M. (2003). Acute liver failure in the United States. *Semin. Liver Dis.* 23, 217-226.
- Lemasters, J. J., Qian, T., Bradham, C. A., et al. (1999). Mitochondrial dysfunction in the pathogenesis of necrotic and apoptotic cell death. *J. Bioenerg. Biomembr.* 31, 305-319.
- Liebler, D. C. and Guengerich, F. P. (2005). Elucidating mechanisms of drug-induced toxicity. *Nat. Rev. Drug Discov.* 4, 410-420.
- Malhi, H. and Gores, G. J. (2008). Cellular and molecular mechanisms of liver injury. *Gastroenterology* 134, 1641-1654.
- McGill, M. R., Yan, H. M., Ramachandran, A., et al. (2011). HepaRG cells: a human model to study mechanisms of acetaminophen hepatotoxicity. *Hepatology* 53, 974-982.
- Narayanan, P. K., Hart, T., Elcock, F., et al. (2003). Troglitazone-induced intracellular oxidative stress in rat hepatoma cells: a flow cytometric assessment. *Cytometry A* 52, 28-35.
- NRC – National Research Council (2007). *Toxicity testing in the 21st century: A vision and a strategy*. Washington DC: National Academies Press.
- O'Brien, P. J., Irwin, W., Diaz, D., et al. (2006). High concordance of drug-induced human hepatotoxicity with *in vitro* cytotoxicity measured in a novel cell-based model using high content screening. *Arch. Toxicol.* 80, 560-604.
- Park, B. K., Kitteringham, N. R., Maggs, J. L., et al. (2005). The role of metabolic activation in drug-induced hepatotoxicity. *Annu. Rev. Pharmacol. Toxicol.* 45, 177-202.
- Pauli-Magnus, C. and Meier, P. J. (2006). Hepatobiliary transporters and drug-induced cholestasis. *Hepatology* 44, 778-787.
- Poli, G. (2000). Pathogenesis of liver fibrosis: role of oxidative stress. *Mol. Aspects Med.* 21, 49-98.



- Reuben, A., Koch, D. G., Lee, W. M., et al. (2010). Drug-induced acute liver failure: results of a U.S. multicenter, prospective study. *Hepatology* 52, 2065-2076.
- Russmann, S., Kullak-Ublick, G. A., and Grattagliano, I. (2009). Current concepts of mechanisms in drug-induced hepatotoxicity. *Curr. Med. Chem.* 16, 3041-3053.
- Sánchez, A., Alvarez, A. M., Benito, M., et al. (1997). Cycloheximide prevents apoptosis, reactive oxygen species production, and glutathione depletion induced by transforming growth factor beta in fetal rat hepatocytes in primary culture. *Hepatology* 26, 935-943.
- Simmons, S. O, Fan, C. Y., and Ramabhadran, R. (2009). Cellular stress response pathway system as a sentinel ensemble in toxicological screening. *Toxicol. Sci.* 111, 202-225.
- Sonich-Mullin, C., Fielder, R., Wiltse, J., et al. (2001). IPCS conceptual framework for evaluating a mode of action for chemical carcinogenesis. *Regul. Toxicol. Pharmacol.* 34, 146-152.
- Spaniol, M., Bracher, R., Ha, H. R., et al. (2001). Toxicity of amiofarone and amiodarone analogues on isolated rat liver mitochondria. *J. Hepatol.* 35, 628-636.
- Terzi, A., Iraz, M., Sahin, S., et al. (2004). Protective effects of erdosteine on rotenone-induced oxidant injury in liver tissue. *Toxicol. Ind. Health* 20, 141-147.
- Turpeinen, M., Tolonen, A., Chesne, C., et al. (2009). Functional expression, inhibition and induction of CYP enzymes in HepaRG cells. *Toxicol. In Vitro* 23, 748-753.
- Uetrecht, J. (ed.) (2010). "Troglitazone", *adverse drug reactions. Handbook of Experimental pharmacology* 196. Berlin, Heidelberg: Springer.
- Waldhauser, K. M., Torok, M., Ha, H. R., et al. (2006). Hepatocellular toxicity and pharmacological effect of amiodarone and amiodarone derivatives. *JPET* 319, 1413-1423.
- WHO Harmonization Project Document (2007). IPCS framework for analysing the relevance of a non-cancer mode of action for human. No. 4, Part 2.
- Xu, J. J., Henstock, P.V., Dunn, M. C., et al. (2008). Cellular imaging predictions of clinical drug-induced liver injury. *Toxicol. Sci.* 105, 97-105.
- Yang, X. X., Hu, Z. P., Chan, S. Y., et al. (2006). Monitoring drug-protein interaction. *Clin. Chim. Acta* 365, 9-29.
- Zhang, X., Liu, F., Chen, X., et al. (2011). Involvement of the immune system in idiosyncratic drug reactions. *Drug Metab. Pharmacokinet.* 26, 47-59.

Acknowledgements

The authors would like to express their gratitude to Dr. Luis Saavedra for his excellent technical assistance with chemical preparation. HepaRG cells are kindly supplied by Dr. Christiane Guguen-Guillouzo (INSERM U522, Hopital Pontchaillou, av. De la Bataille, F-35033 Rennes, France) and used under a Material Transfer Agreement between INSERM U522 and the Institute of Health and Consumer Protection (DG JRC, Ispra, Italy). We thank Dr. Anne Milcamps for providing editorial review.

Correspondence to

Milena Mennecozzi, PhD
Systems Toxicology Unit
Institute for Health and Consumer Protection
JRC – European Commission
Via E. Fermi 2749 TP202
21027 Ispra (VA), Italy
Phone: +39 0332 786785
Fax: +39 0332 789963
e-mail: milena.mennecozzi@ec.europa.eu